Materials and Structures (2017) 50:163
DOI 10.1617/s11527-017-1032-8

ORIGINAL ARTICLE

Numerical simulation of self-consolidating concrete flow as a heterogeneous material in L-Box set-up: coupled effect of reinforcing bars and aggregate content on flow characteristics

Masoud Hosseinpoor · Kamal H. Khayat · Ammar Yahia

Received: 25 August 2016 / Accepted: 4 April 2017 / Published online: 7 April 2017

Abstract A computational fluid dynamics software was employed to simulate the coupled effect of reinforcing bar spacing and coarse aggregate content on the blocking resistance and shear-induced segregation of self-consolidating concrete (SCC) along the horizontal channel of the L-Box apparatus. The rheology of the modelled suspending fluid, which corresponds to the stable and homogeneous portion of the mixture, consists of plastic viscosity value of 25 Pa s, yield stress values of 75 Pa, fluid density of 2500 kg/m^3, and shear elasticity modulus value of 100 Pa. Two different values of 20-mm spherical particles (135 and 255 particles in total), as well as three bar arrangements consisting of 0, 3, and 18 bars distributed along the horizontal channel of the L-Box were considered in the numerical simulations. A new approach is proposed to evaluate the coupled effect of reinforcing bar arrangements and the number of spherical particles on the flow performance of SCC.

M. Hosseinpoor · A. Yahia
Department of Civil Engineering, Université de Sherbrooke, Sherbrooke, QC J1K2R1, Canada

K. H. Khayat (✉)
Department of Civil, Architectural and Environmental Engineering, Missouri University of Science and Technology, Rolla, MO 65409-0710, USA
e-mail: khayatk@mst.edu

Keywords Blocking · Dynamic segregation · Flow simulation · Heterogeneous analysis · L-Box test · Self-consolidating concrete

1 Introduction

Recently, there has been a great interest in using self-consolidating concrete (SCC) in cast-in-place and precast construction as a new class of high performance concrete. The highly flowable nature of SCC facilitates the casting process and reduces the placing energy and workforce requirement compared to conventional vibrated concrete. The high filling capacity of SCC makes it ideal for casting densely reinforced structural members to pass through the narrow gaps in the formwork. In doing so, the material should maintain homogeneous distribution of the coarse particles in the mortar matrix [1, 2]. In order to achieve higher flowability and passing ability, the rheological parameters of SCC, such as yield stress and plastic viscosity, should be significantly less than conventional concrete. For example, typical ranges of plastic viscosity and yield stress for conventional concrete are 500–2000 Pa s and 50–100 Pa, respectively, while those corresponding to SCC are 0–100 Pa s and 0–80 Pa, respectively [3]. In a given coarse particle content, the lower rheological parameters for SCC are due to its highly flowable paste and mortar matrix which surround the coarse particles in a

stable concrete suspension system. Accordingly, due to the low values of viscosity and yield stress of mortar in SCC and high flow kinetic energy required for casting of such SCC, there is an increased risk of separation of coarse particles from the suspending fluid (mortar), during the flow (i.e., blocking and shear induced segregation) or thereafter when the material is at rest (i.e., static segregation). Greater risk of dynamic segregation can be due to lower drag forces exerted on coarse particles to maintain them homogenously distributed in the suspension system. Therefore, the investigation of the interaction of reinforcement bar spacing and coarse particle concentration in mortar systems of various rheological properties can enable the evaluation of the dynamic performance of the SCC during the casting process [4].

Dynamic segregation can increase when SCC flows over a long distance or in the presence of obstacles (i.e., risk of blockage affecting the passing ability characteristics of the concrete). Passing ability refers to the ability of the concrete to pass through narrow gaps between various obstacles, such as reinforcing steel, to hold the aggregates in the suspension and, consequently, maintain its homogeneity [5–7]. Therefore, comparing the properties of the final profiles through the flow path (in horizontal and vertical directions) and also, in the locations around the obstacles (i.e., reinforcement bars) can enable the evaluation of dynamic stability and blocking resistance of SCC, respectively. This can be carried out using empirical and theoretical tools.

As an empirical tool, the L-Box test is often employed to evaluate the restricted flow of SCC in the presence of obstacles and evaluate the passing ability and dynamic segregation of the suspension [8]. The L-Box set-up consists of vertical and horizontal compartments separated by a diving door that slides up enabling the material cast in the vertical compartment to flow gravitationally into the horizontal channel. Limited studies have been conducted to investigate the relationship between the rheological parameters of SCC and the various responses that can be determined using the L-Box test [9, 10]. Turgut et al. [11] developed a modified L-Box set-up to evaluate dynamic segregation of SCC at different locations in the horizontal channel. Nepomuceno et al. [12] proposed semi-empirical models to optimize the maximum aggregate volume fraction to achieve a proper passing ability of SCC under different flow restrictions and bar spacings. Yahia et al. [13] developed statistical models to evaluate the coupled effect of mix design and rebar spacing on the passing ability of SCC using a modified L-Box test setup.

Numerical simulations have been employed recently as theoretical tools to predict dynamic stability and passing ability of SCC [4, 14–19]. The numerical modeling of fresh SCC flow should take into account the interaction between the aggregates, the suspending fluid (i.e., cement paste/mortar), the configuration of the reinforcement, and the formwork wall characteristics [4, 14–16]. Vasilic et al. [20] evaluated numerically the effect of presence of reinforcing obstacles as a porous medium on passing ability of SCC, considered as a single homogeneous fluid. Spangenberg et al. [18] studied flow induced particle migration in SCC and showed that in the case of industrial casting of SCC, gravity induced particle migration dominates all other potential sources of dynamic segregation induced by the flow of SCC into place. Spangenberg et al. [19] investigated different patterns of dynamic segregation during casting of SCC using experimental tests and numerical simulations. They showed that gravity induced particle migration has dominant effect on the coarsest particles resulting in a decrease of coarse aggregate content along the horizontal distance from the casting point and also in the vertical direction at the top layer of the concrete.

In this paper, a computational fluid dynamics (CFD) software was employed to simulate free surface flow of SCC in the L-Box test apparatus. The Navier–Stokes and conservation of mass equations for incompressible materials are solved by the volume of fluid (VOF) method [21]. In total, six simulations were carried out to study the effect of reinforcing bar spacing and aggregate particle content on the resistance to blocking and shear-induced dynamic segregation of SCC in the horizontal and vertical directions along the horizontal leg of the L-Box apparatus.

The investigation considered one suspending fluid that corresponds to a stable and homogeneous portion of an SCC mixture. This suspending fluid includes the fraction of the coarse and fine aggregates that can be rather homogeneous during the casting process. The investigated suspending fluid (i.e., the stable fraction of the SCC mixture) has a moderate plastic viscosity, a high yield stress, and a similar density as the suspended particles (large coarse aggregate fraction) in order to minimize gravity induced segregation.

Segregation and blocking phenomena are only calculated for two contents of suspended coarse aggregates, which are less than typical contents of coarse aggregates in SCC (i.e., 10%–30%). Indeed, it was assumed that the finer coarse aggregate fraction that can remain in homogeneous suspension in the SCC mixture during the flow period are a part of the suspending fluid. Accordingly, the suspending fluid can be assumed as the stable portion of the SCC mixture. It can be explained by the fact that segregation and blocking do not occur for all the aggregates of the concrete suspensions, but only for a portion of them, having larger sizes (20 mm). On the other hand, due to the limits in calculation capacity, tracking of the positions of all the coarse aggregate particles (having typical contents and sizes, ranging from 10% to 30% and 5 to 20 mm, respectively) would have been impossible. Accordingly, two different initial suspended mono-size (20 mm) particle contents and three distributions of reinforcing bar obstacles were simulated to evaluate the coupled effect of reinforcing bars and particle loading on the flow performance of SCC. The paper discusses the results of the numerical simulation in terms of flow profiles, and particle distribution throughout the L-Box channel (horizontal direction) and fluid depth (vertical direction) for a given period of flow time.

2 Properties of modelled materials

The investigated parameters of the CFD modeling that were considered included a plastic viscosity of 25 Pa s, a yield stress of 75 Pa, a shear elasticity modulus of 100 Pa, as well as a density of the suspending fluid of 2500 kg/m^3. The shear elasticity modulus is the ratio of shear stress to shear strain in the elastic state of the fluid, which is before the beginning of the plastic state. The modelled suspensions included the introduction of 135 and 255 spherical particles measuring 20 mm of diameter. This corresponds to particle contents of 4.6% and 8.7%, by volume, and was done to study the effect of coarse particle content on shear-induced segregation of the investigated SCC mixtures. The particles have the same density as the suspending fluid (i.e., 2500 kg/m^3) to minimize gravity induced segregation.

The L-Box set-ups included three bar arrangements placed immediately downstream from the sliding gates with different bar spacing and densities. In order to evaluate the pure particle content effect on non-restricted dynamic stability, two simulations were carried out in the absence of obstacles. Two other simulations included the use of three standard bars measuring 12 mm in diameter and 200 mm in height that are located right after the gate separating the vertical and horizontal compartments of the L-Box. In addition, 18 bars consisting six rows of three bars positioned at 100-mm spacings distributed along the horizontal channel were modelled. These models included two different particle contents. The schematics of the L-Box set-up and configuration of the obstacles are presented in Fig. 1.

3 Numerical simulation and boundary conditions

A CFD software (FLOW3D®) was employed to simulate free surface flow of the SCC in the L-Box test apparatus. The basic equations of the conservation of mass for incompressible materials and the Navier–Stokes equations are solved by the Volume of Fluid (VOF) method [21]. In total, six simulations were carried out for a period of flow of 6.4 s, which was found to be the maximum duration needed to empty the SCC from the vertical leg of the L-Box for the investigated rheological properties investigated earlier by the authors [22]. In order to discretize the geometry, solid elements, and suspension, two mesh blocks of 326,832 cells with 5-mm size in the x, y, and z directions were created.

The Dirichlet–Neumann boundary conditions were imposed to the flow domain based on the geometry of the L-Box; the velocity of the walls and the gate rising rate were set to zero and 0.03 m/s, respectively, as indicated in Fig. 2. The friction boundary conditions were assumed between particles, fluid, and the walls of the apparatus with a friction coefficient value of 0.4 [23]. The modelled fluids are considered as Non-Newtonian Bingham fluids using an elasto-viscoplastic model with implicit numerical approximation. Gravity stresses are calculated using gravitational acceleration value of 9.81 m/s^2.

In order to simulate the motion of moving boundaries and distinct entities, such as the gate of the L-Box and suspended particles in the heterogeneous simulations, a General Moving Object (GMO) technique is employed. A GMO is a rigid body under any

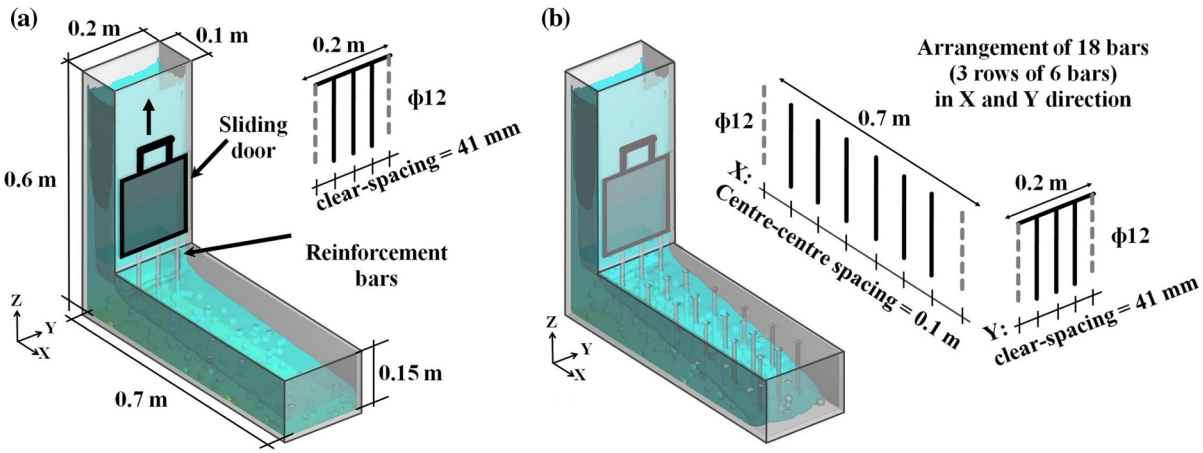

Fig. 1 **a** Schematics of the L-Box set-up and configuration of standard 3 bars after the sliding door, **b** 18 bars

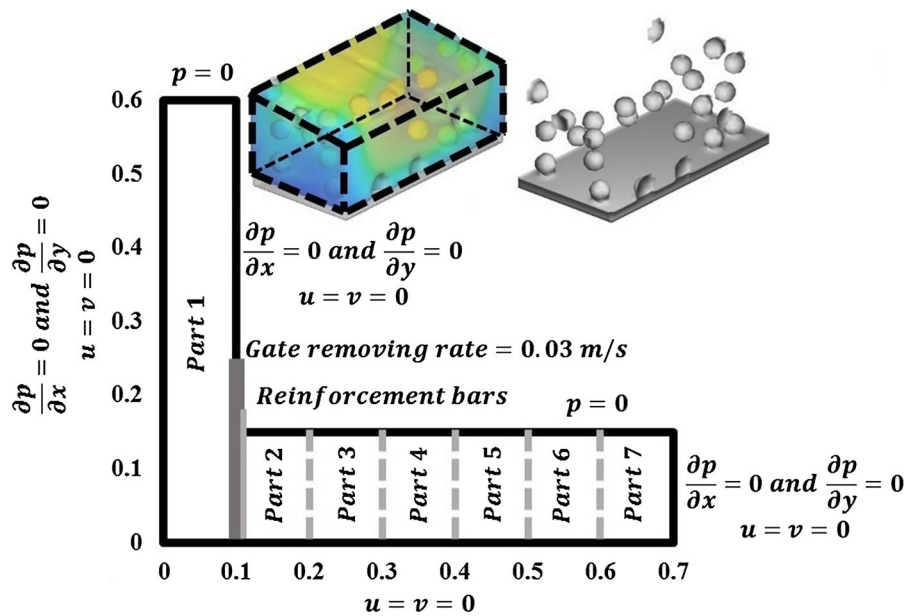

Fig. 2 Boundary conditions and horizontal sampling sections

type of physical motion which is either dynamically coupled with fluid flow or prescribed. It can move with six degrees of freedom or rotate around a fixed point or a fixed axis. The GMO model allows to have multiple moving objects in one problem, and each moving object can have any independently defined type of motion. GMO components can be of a mixed motion type, such as translational and/or rotational velocities that are coupled in some coordinate directions and prescribed in the other directions. A body-fixed reference system (body system), defined for each moving object, and the space reference system (space system) are employed. At each time step, the hydraulic force and torque due to pressure, gravitational, and shear stresses are calculated, and equations of motion are solved for the moving objects under coupled motion with consideration of hydraulic, gravitational, shear forces, and torques. Area and volume fractions are recalculated at each time step based on updated object locations and orientations. Source terms are added in the continuity equation and the VOF transport equation to account for the effect of moving objects to displace the fluid. The tangential velocity of the moving object boundaries is introduced into shear stress terms in the momentum equation. Implicit numerical method is employed to calculate iteratively

coupling of fluid flow and GMO motion in each time step, using the force and velocity data from the previous time step [24].

In order to consider particle–particle, particle–obstacle, and particle–wall interactions, a coefficient of restitution of 0.8 was applied for collision physical model. The modelled flow is assumed to be a laminar flow type [25]. It is worthy to mention that numerical simulations carried out on an i7-2600 CPU 3.40 GHz processor required a total running times between 60 and 135 h per simulation. The running times depended mostly on the number of the particles and obstacles. In total, six simulations were require to complete the investigation.

3.1 Sampling methods and anticipated results

In order to evaluate flow performance of the modelled suspensions, the simulated flow profiles were calculated at 0.1-s time steps. Blocking resistance and dynamic stability properties of the suspensions in the horizontal direction were calculated by measuring the volumetric particle contents across seven 10-cm long sections located along the horizontal channel of the L-Box, as illustrated in Fig. 2. The number and position of the particles, as well as the volume of the fluid in each section were calculated at each 0.1-s time steps.

On the other hand, dynamic stability of the suspensions in vertical direction was evaluated by comparing the volumetric particle contents across three vertical layers (bottom, middle, and top) measured at the end of the flow period (i.e., $t = 6.4$ s). As presented in Fig. 3, the thicknesses of the bottom and middle layers are 3 cm, and the remaining thickness ($Z > 6$ cm) corresponds to the top layer.

4 Results and discussion

4.1 Effect of particle contents on passing ability and dynamic stability of suspensions in horizontal direction

By calculating the fluid volumes and particle contents in two extreme horizontal sampling sections that are located behind the bars (part 1) and at the end of the horizontal channel of the L-Box (part 7), the extremity horizontal dynamic segregation index (E.H.D.S.I.) can be defined in various durations that can be calculated at frequencies of 0.1 s. The E.H.D.S.I. can be calculated as:

$$\text{E.H.D.S.I.} = \frac{\text{Particle content @ part 1} - \text{Particle content @ part 7}}{\text{Initial mean particle content}} \quad (1)$$

The values of E.H.D.S.I. index show the dispersions in particle content of the reference mixture, measured at two extreme parts of the horizontal channel, as a result of horizontal dynamic segregation. In order to evaluate the effect of particle contents on the non-restricted dynamic segregation of suspension (i.e., dynamic segregation in the absence of the obstacles), values of E.H.D.S.I. are calculated for two suspension consisted of two different initial particle contents (4.6% and 8.7%, by volume of concrete) and presented in Fig. 4. The L-Box set-up for these simulations did not consider the presence of any reinforcement bars in the horizontal channel of the L-Box to evaluate the pure particle effect on the flow performance of SCC.

As can be observed in Fig. 4, for both particle contents, the E.H.D.S.I. values increased with time to maximum values then decreased. The ascending parts of the curves can be related to the period that the vertical compartment of the L-Box is not completely empty (i.e., the flow times from 0 to almost 2.5–3 s) where particles are of greater concentration in part 1 with less velocity than the suspending fluid. As can be observed in this initial flow period, the values of E.H.D.S.I. obtained for both particle contents are comparable. It can be due to the comparable friction and drag forces exerted on the particles, where friction coefficients, particle sizes, velocity magnitudes, and plastic viscosity values of the suspending fluids were similar in this period. On the other hand, the behavior of suspensions in the descending part of the curve (i.e., flow times $t > 3$ s) can be explained by the flowability of the mixtures which can push the accumulated particles to move ahead and reach the end of the horizontal channel (part 7). However, in this period, the suspension with the higher particle content of 8.7% exhibited greater E.H.D.S.I. values than the simulated SCC with the lower particle content of 4.6%. This can be due to the higher lattice effect [26–28] of the particles, which were already segregated during the first period (i.e., $0 < t < 3$ s), on the motion of the

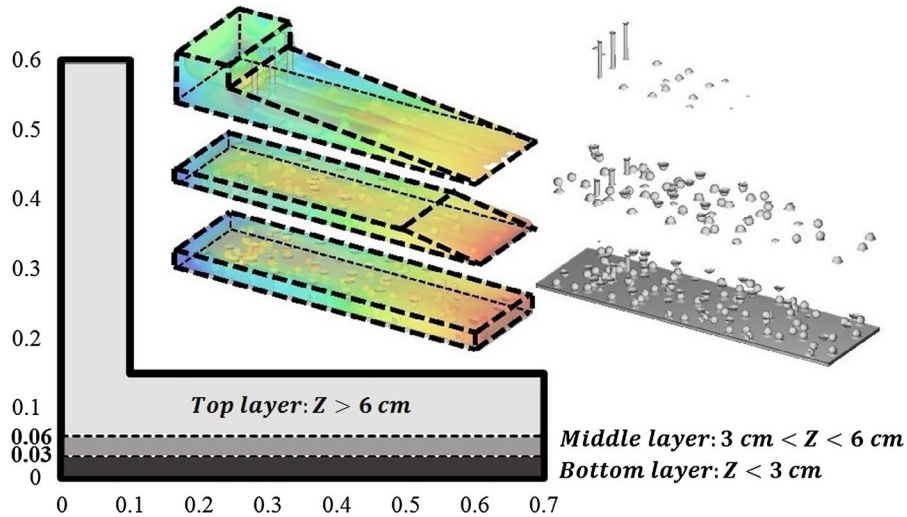

Fig. 3 Vertical sampling layers

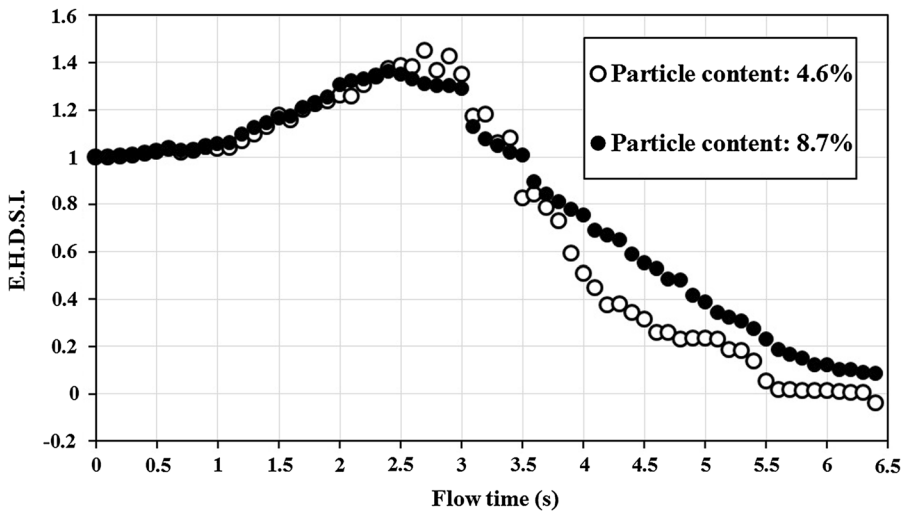

Fig. 4 Variations of E.H.D.S.I. index values with flow time determined at 0.1 s intervals

particles towards the end of channel (part 7). The lattice effect corresponds to the internal structure of the segregated particles. This structure can reduce the displacements of the particles, whether inside the lattice network, or the upcoming particles from the vertical compartment of the L-Box.

Shear-induced dynamic segregation of the mixtures throughout the horizontal direction can be evaluated by calculating the maximum horizontal dynamic segregation indices for each horizontal sampling part (i = 1–7) individually in the whole period of the flow (i.e., t = 0–6.4 s), as follows:

$$\text{I.H.D.S.I.}\,(i) = \text{Maximum}\left(\frac{\text{Particle content @ part}\,(i) - \text{Particle content @ part 7}}{\text{Initial mean particle content}}\right) \quad (2)$$

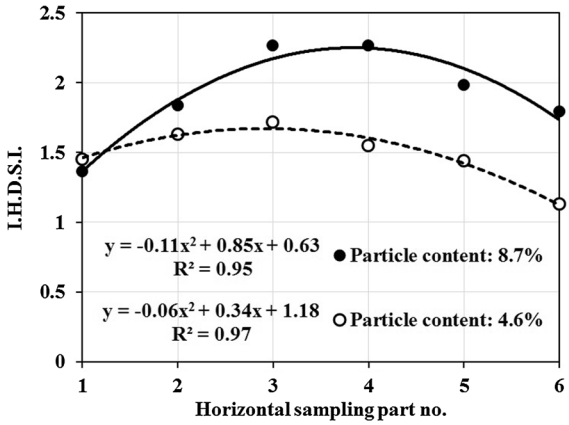

Fig. 5 Variations of I.H.D.S.I. index values with horizontal sampling part number (L-Box with no obstacles)

where I.H.D.S.I. (i) is the individual horizontal dynamic segregation index, obtained in the horizontal sampling part i. By comparing the results of the I.H.D.S.I. values for the horizontal samples $i = 1$–6, the variation of segregations of the particles along the horizontal direction can be evaluated. The results of the simulations, corresponded to the L-Box set-up which does not consist any obstacle are presented in Fig. 5.

As can be observed in Fig. 5, the simulated suspensions made with both particle contents of 4.6% and 8.7% exhibited maximum I.H.D.S.I. values in the third horizontal sampling part. Therefore, the particles segregate mostly in a distance of 0.2 m after the sliding door in the horizontal channel, which means the first 1/3 of the 0.6 m horizontal leg. On the other hand, the suspension with higher particle content of 8.7% exhibited higher I.H.D.S.I. values compared to those obtained by particle content of 4.6%. This can be called as the effect of the "particle–particle interactions" on horizontal dynamic stability of the suspensions. By increasing the particle content, the probability of formation and also strength of the internal structure of segregated particles (i.e., the lattice effect) in horizontal direction increase. This can reduce the relative horizontal displacements of the particles to the suspending fluid, in the case of the higher particle content suspension. For example, an increase in particle content from 4.6% to 8.7% can lead to the maximum increase of 0.71 (from 1.55 to 2.26) in I.H.D.S.I. values in part 4, which corresponds to the horizontal sampling portion located at a distance of 0.2 m from the sliding door.

However, in part 1 (located in vertical compartment of the L-Box), the suspension with higher particle content of 8.7% showed slightly (0.09) lower I.H.D.S.I. value than the SCC with the lower particle content (4.6%). This can be explained by the fact that unlike the horizontal channel, the major direction of the flow in part 1 is vertical and towards gravity (Z direction). This is due to the geometry of the apparatus, as well as the confinement of the flow by the side walls, in both X and Y directions. On the other hand, as observed earlier in Fig. 4, the suspensions reach their maximum E.H.D.S.I. values (which is equal to the I.H.D.S.I. value in part 1) in the period of flow time that the vertical part of the L-Box is not completely empty and suspension still flows down. Therefore, the lattice forces of the particles, which are located in the vertical compartment of the L-Box, are in the same direction of the flow, as well as the gravitational forces. Indeed the particles in the upper vertical levels push the particles of the lower levels to travel from the vertical part of the L-Box towards the horizontal channel. This effect can increase in the case of presence of higher numbers of particles in the vertical parts. Therefore, it can be concluded that in the vertical compartment of the L-Box (i.e., part 1), the lattice structure of the particles has an auxiliary effect on displacement of the particles, which can decrease the I.H.D.S.I. values for the suspensions having greater particle content.

The results of the calculated values of I.H.D.S.I. for the L-Box set-ups consisting of 3 and 18 reinforcing bars along the horizontal leg are presented in Fig. 6a, b, respectively. Similar to the non-restricted flow of the suspension presented in Fig. 5, increasing the particle content can increase the I.H.D.S.I. values for the L-Box set-ups consisting of 3 and 18 obstacles along the horizontal leg. For example, in the case of presence of 18 bars through the horizontal channel, the maximum increase of 2.47 in I.H.D.S.I. values (from 2.70 to 5.17) is obtained in the part 5. As stated earlier, this can be due to the negative effect of the lattice structure of segregated particles in the horizontal leg of the L-Box on the displacement of upcoming particles towards part 7.

On the other hand, as can be observed in Fig. 6, in presence of 3 and 18 bars, increasing the particle content can decrease slightly the I.H.D.S.I. values by 0.07 and 0.03, respectively, in part 1. As explained earlier, this can be due to the auxiliary effect of the

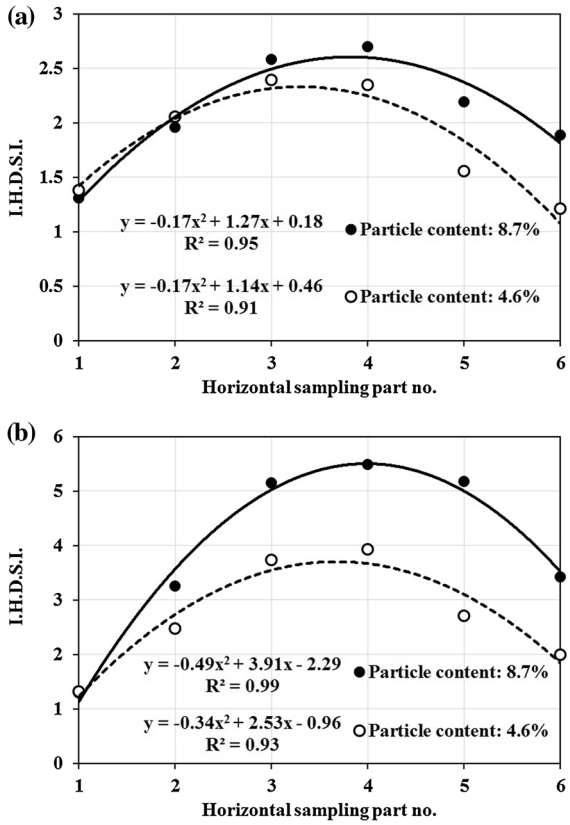

Fig. 6 Particles effect: values of I.H.D.S.I. for suspensions with different particle contents versus horizontal sampling location along the L-Box with **a** 3 and **b** 18 reinforcing bars in the horizontal channel

lattice performance of particles in the vertical compartment of the L-Box on the displacement of the particles in lower levels.

It is worthy to mention that the values of I.H.D.S.I. (i) for the L-Box set-up (Eq. 2) with 18 bars, can also be used to evaluate the passing ability of the suspension for each row (i.e., $i = 1$–6) of obstacles. Indeed, by calculating the I.H.D.S.I. (i) values, the passing ability of the suspension through each row of reinforcement bars (i between 1 and 6) can be evaluated. This can be calculated by the ratio of difference of particle contents at the part located behind that row (part (i)) and the last part (i.e., part 7) to initial particle content. Therefore, the I.H.D.S.I. values for 18 bars L-Box set-up can be used as the maximum blocking index values (i.e., $B.I._{max}$). As can be observed in Fig. 6b, for both initial particle contents of 4.6% and 8.7%, the maximum I.H.D.S.I. = $B.I._{max}$ values of 3.93 and 5.48 were obtained, respectively, right behind the $i = 4$th row of reinforcement bars, which is located at the distance of 0.3 m from the sliding gate of the L-Box. This means that suspensions segregate mostly in the first half of the horizontal channel (i.e., 0.6 m long leg).

4.2 Effect of reinforcement bars on passing ability and dynamic stability of suspensions in the horizontal direction

In order to evaluate the effect of reinforcement bars (obstacles) on dynamic stability and blocking resistance of the investigated SCC, the results of simulated values of I.H.D.S.I. are compared for different number of obstacles (i.e., 0, 3, and 18) along the horizontal channel of L-Box. These comparisons are presented for the suspensions with two different particle contents of 4.6% and 8.7% and presented in Fig. 7a, b, respectively.

As can be observed in Fig. 7a, b, for both particle contents of 4.6% and 8.7%, the simulations showed minimum (1.71 and 2.26, respectively) and maximum (3.93 and 5.48, respectively) values of I.H.D.S.I. for the L-Box set-ups consisted of 0 (i.e., non-restricted flow) and 18 bars along the horizontal channel, respectively. It can be referred to the bar effect on flow performance of the investigated suspensions. This can be explained by the fact that increasing the number of obstacles can restrict the flow space needed for the particles to move freely and, consequently, it can increase the collisions and frictional stresses between the particles and obstacles. Therefore, increasing the number of obstacles in the horizontal direction can restrict the horizontal displacement of the particles. However, as can be observed in Fig. 7, increasing the number of obstacles (i.e., from 0 to 18) does not show any significant effect (i.e., a decrease of 0.08 from 1.36 to 1.28) on I.H.D.S.I. in part 1, compared to other parts. This is due to the fact that unlike the horizontal leg, the flow in vertical part of the L-Box (part 1) is non-restricted. Therefore, lattice effect of particles, which are placed in the vertical part, on displacement of the particles is more dominant than the effect of configuration of obstacles in the horizontal channel. For a given particle content, the lattice effect of the particles in the non-restricted part 1 are comparable and, consequently, the suspension shows comparable I.H.D.S.I. values in this part, regardless of number of obstacles in the restricted parts.

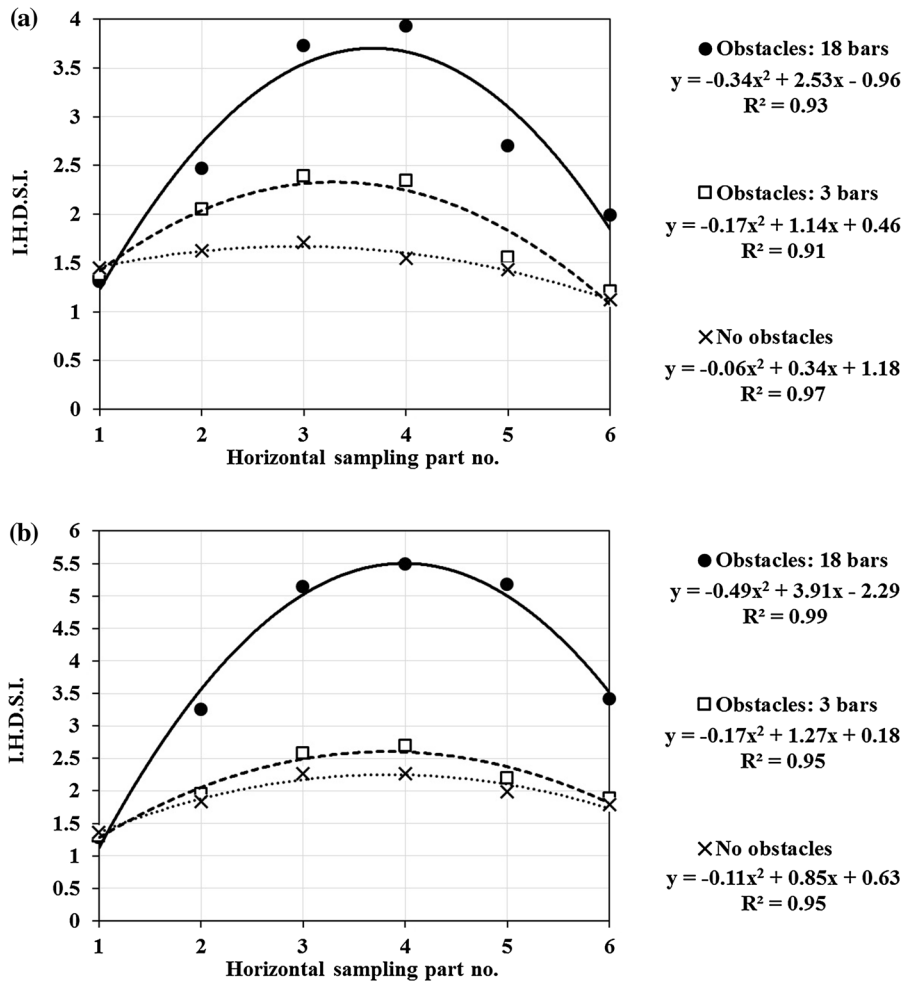

Fig. 7 Bar effect: variation of I.H.D.S.I. values in different horizontal sampling parts for different configurations of obstacles, obtained for values of particle content of **a** 4.6% and **b** 8.7%

Furthermore, as explained earlier, the results presented for I.H.D.S.I. values of the L-Box set-up consisted of 18 bars along the horizontal leg, can be used to evaluate the passing ability of the suspensions through each row of reinforcing bars. On the other hand, the suspensions showed their maximum I.H.D.S.I. (or $B.I._{max}$) values in the part 4. As can be observed in Fig. 7, for part 6, compared to the middle parts 4 and 5, the bar effect on I.H.D.S.I. values decrease. For example, in the case of the suspension with 8.7% particle content, increasing the number of obstacles from 0 to 18, can increase I.H.D.S.I. values in parts 4 and 6 from 2.26 to 5.48 (an increase of 3.22), and from 1.79 to 3.41 (increased by 1.62), respectively. Therefore, it can be concluded that the bar effect on dynamic segregation in the middle parts are higher than those which are located in the terminal part 6, right behind the part 7. It is due to the higher particle content observed in the middle sections (according to higher I.H.D.S.I. values) compared to part 6. This can increase the probability of the formation of particle blocking arcs and the friction between the particles and obstacles in these parts. The effect of the interactions, observed between the coarse particles and the reinforcement bars, on dynamic stability and blocking resistance of the suspensions is called "bar–particles coupled effect", and will be discussed in the next section.

4.3 Bar–particles coupled effect on flow performance of suspensions in the horizontal direction

In order to evaluate the effect of interactions between the particles and the reinforcing bar obstacles, two new indices are defined. These indices include the

particle content effect (P.C.E.) and bar effect (B.E.) in different horizontal sampling parts ($i = 1$–6), as follows:

$$\text{P.C.E.}_{(i,j,k)} = \frac{\text{I.H.D.S.I.}_{(i,j)} \text{ for particle content value of } k = 8.7\%}{\text{I.H.D.S.I.}_{(i,j)} \text{ for particle content value of } k = 4.6\%} \quad (3)$$

$$\text{B.E.}_{(i,j,k)} = \frac{\text{I.H.D.S.I.}_{(i,k)} \text{ for } j = 18 \text{ bars along the horizontal channel}}{\text{I.H.D.S.I.}_{(i,k)} \text{ for } j = 3 \text{ bars along the horizontal channel}} \quad (4)$$

where $\text{P.C.E.}_{(i,j,k)}$ and $\text{B.E.}_{(i,j,k)}$ are the indices of the particle content effect and bar effect on flow performance of the suspensions made with particle content k ($k = 4.6\%$ and 8.7%), in the L-Box set-up consisting of j number of reinforcing bars ($j = 3$ and 18). These indices are calculated for the sampling part i ($i = 1$–6). The P.C.E. index in each sampling part ($i = 1$–6) is calculated as the ratio of I.H.D.S.I. values obtained for suspensions with particle content (k) of 8.7% to those values obtained for k of 4.6%. On the other hand, the B.E. index in each horizontal part ($i = 1$–6) is calculated by the ratio of the I.H.D.S.I. values obtained for the L-Box set-up consisting of $j = 18$ bars in the horizontal channel to the values obtained for a $j = 3$ bars L-Box set-up. Comparing the values of $\text{P.C.E.}_{(i,j,k)}$ and $\text{B.E.}_{(i,j,k)}$ in different horizontal parts ($i = 1$–6), in the presence of different number of bars ($j = 3$ and 18) along the horizontal channel, and different particle content ($k = 4.6\%$ and 8.7%), respectively, can enable the evaluation of the coupled effect of reinforcing bar–particle on flow performance of the investigated suspensions in the horizontal direction of the L-Box. The results of these comparisons are presented in Fig. 8.

As can be observed in Fig. 8, the particle content (P.C.E.) and bar (B.E.) effect indices are found to be more than value of 1 in different horizontal sampling parts ($i = 2$–6). Therefore, it can be concluded that increasing both the particle content and number of obstacles can increase the I.H.D.S.I. values (leading to greater horizontal dynamic segregation). On the other hand, the maximum values of P.C.E. of 1.91 and B.E. of 2.36 were obtained for the highest congested flow ($j = 18$ bars) and the suspension with the highest particle content ($k = 8.7\%$), respectively. This can be explained by the fact that increasing the number of reinforcement bars and the number of particles can increase the probability of formation of the blocking arcs, due to higher particle-bars interactions, which means higher friction and collision between the particles and the obstacles.

Furthermore, as can be observed in Fig. 8, once the distance from the vertical compartment of L-Box increases (i.e., part 1 to part 6) the P.C.E. and B.E. values for lower number of obstacles ($j = 3$ bars) and the suspension made with lower particle content ($k = 4.6\%$), increase continuously from 0.95 to 1.56 (an increase of 0.61) and from 0.95 to 1.65 (increased by 0.70), respectively. Similarly, P.C.E. and B.E. values for higher number of obstacles ($j = 18$) and the suspension with higher particle content ($k = 8.7\%$) increase from 0.98 to 1.91 (an increase of 0.93) and from 0.98 to 2.36 (increased by 1.38) with the distance from the vertical compartment (part 1) up to the part 5 (i.e., higher horizontal part number), respectively. This increment in particle and bar effects, obtained by higher horizontal sampling part number can be explained by the fact that in a higher distance from the vertical compartment, the auxiliary lattice effect of the particles located in the vertical part of the L-Box on displacement of the particles in horizontal channel decrease. This is due to dissipation of flow energy, according to the flow surface level descend in the vertical part and consequently, lower gravitational forces. On the other hand, in the horizontal channel, both bar and lattice effect of the segregated particles are in the same direction to resist against the displacement of the particles. This can be more dominant in presence of higher number of bars and the suspensions with higher particle contents, due to higher interactions between the bars and particles. However, once the suspensions segregate mostly in the mid parts of the horizontal channel, accordingly, due to lower particle content in the part 6, the probability of bar–particle interactions (i.e., collision and friction) and, consequently, formation of blocking arcs decrease. Accordingly, as can be observed in Fig. 8a, b, P.C.E. and B.E. values for higher number of obstacles ($j = 18$) and the suspension made with higher particle content ($k = 8.7\%$) decrease in part 6 compared to part 5 from 1.91 to 1.71 (a decrease of 0.20) and from 2.36 to 1.81 (decreased by 0.55), respectively.

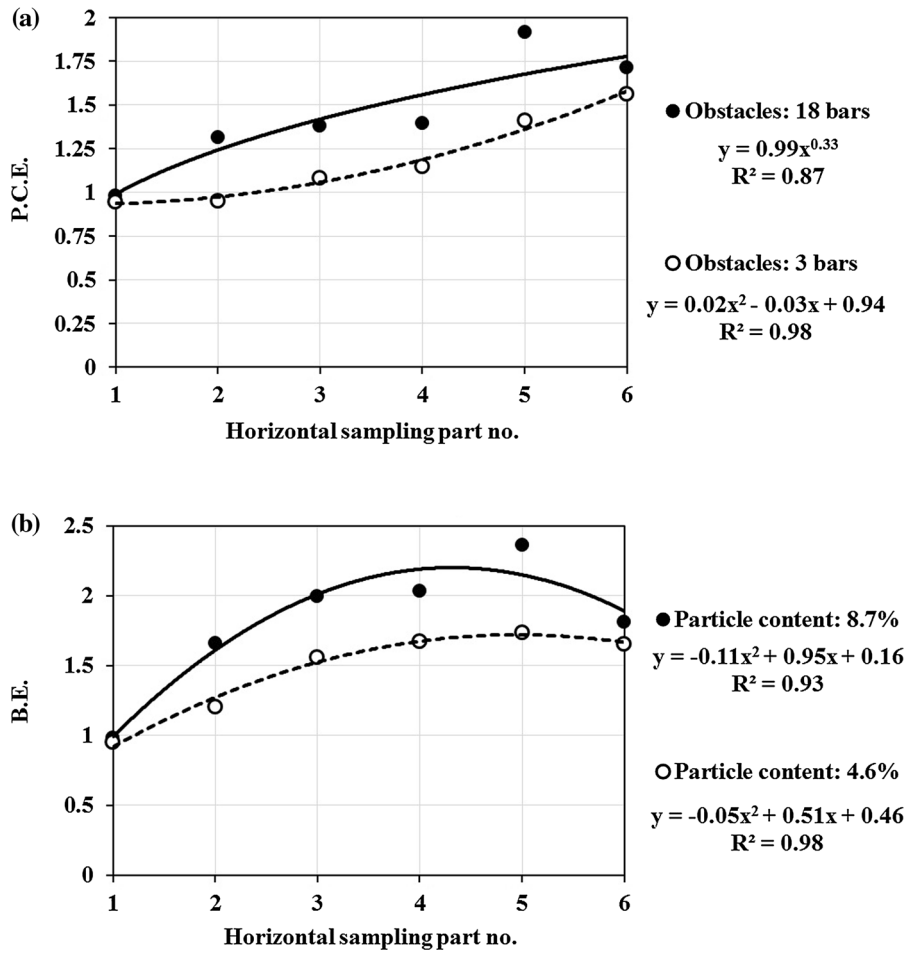

Fig. 8 Bar–particles coupled effect on flow performance of the investigated suspensions in different horizontal sampling parts $i = 1$–6: **a** variation of particle content effect (P.C.E.) for two different number of obstacles $j = 3$ and 18, and **b** variation of bar effect (B.E.) for two different particle contents of $k = 4.6\%$ and 8.7%

Calculating the fluid volume and particle content in each of the seven horizontal sections along the horizontal leg of the L-Box, shear-induced dynamic segregation of the mixtures in the horizontal direction can be quantified for each 0.1-s time step by coefficient of variation of particle contents in all the seven horizontal parts (parts 1–7), as follows

$$\mathrm{COV} = \frac{\text{Standard deviation of particle contents (parts } 1, 2, 3, 4, 5, 6, \text{ and } 7)}{\text{Average of particle contents (parts } 1, 2, 3, 4, 5, 6, \text{ and } 7)} \quad (5)$$

The bar–particle coupled effects on dynamic stability of the suspensions are then evaluated by comparing the ratio of COV values corresponding to 18 bars configuration L-Box to those values obtained in presence of 3 bars obstacles, for both 4.6% and 8.7% particle content suspensions, in the whole period of flow (i.e., $t = 0$–6.4 s). These results are presented in Fig. 9. As can be observed, scattering of the data points from lines $x = 1$ and $y = 1$ can indicate the effect of increasing the number of obstacles (from 3 to 18) on horizontal dynamic segregation. On the other hand, the effect of higher particle content (from 4.6% to 8.7%) on horizontal dynamic segregation can be evaluated by the dispersion of the data points from the line $y = x$.

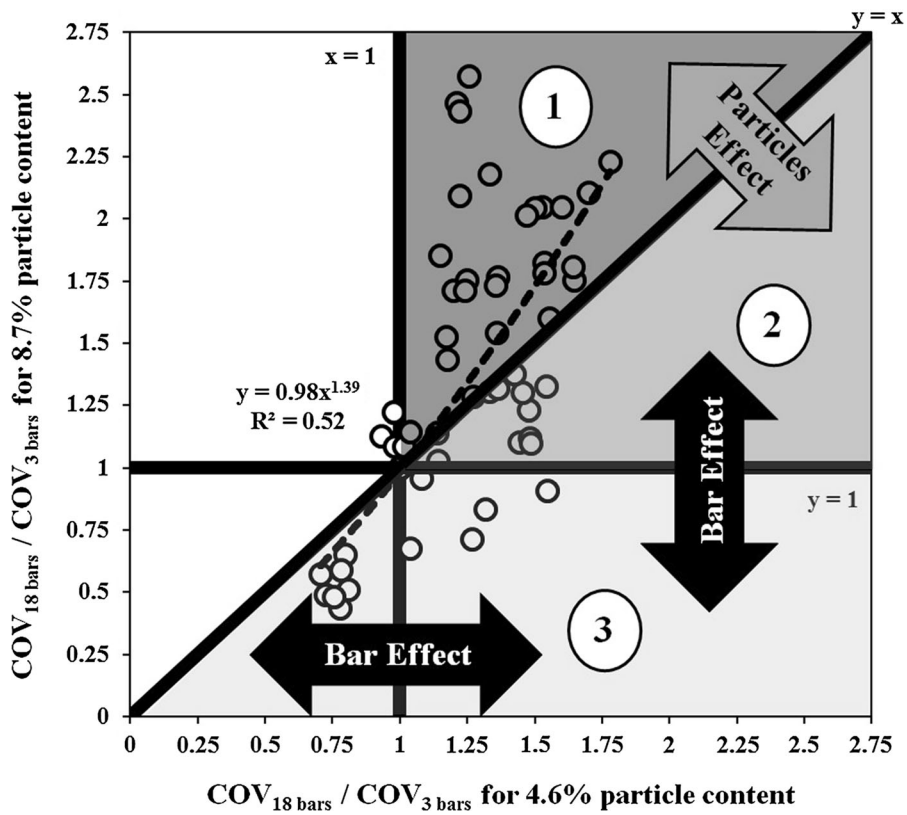

Fig. 9 Variation of bar–particles coupled effect with dynamic stability of investigated mixtures

According to data presented on Fig. 9, the bar–particles coupled effect can be described by three different zones, as follows:

1. Bar–particle parallel effect, zone 1: This zone is limited to the area surrounded by $x > 1$ and $y > x$. In this part, increasing both the number of bars and initial particle contents can result in greater blocking and dynamic segregation. This can be due to the formation of particle blocking arches behind the bars. In this part, both the presence of bars and particle content have dominant effects on this phenomena.
2. Bar–particle opposite effect, zone 2: This zone is limited to the area surrounded by $y > 1$ and $y < x$. In this zone, increasing the number of bars can result in more blocking and dynamic segregation due to greater risk of blocking arch formation. On the other hand, increasing the particle content can improve the dynamic stability and passing ability of the suspension. Such better homogeneous behavior can be explained by particle effects on increasing the overall viscosity and yield stress of the suspension, which leads to a lower fluid deformation and, therefore, less dynamic segregation. In this zone, the presence of bars has more dominant effect.
3. Bar–particle opposite effect, zone 3: This zone is limited to the area surrounded by $y < 1$ and $y < x$. In this part, increasing the particle content can decrease the additive effect of bars on blocking and dynamic segregation by increasing the overall viscosity and yield stress of the suspension. In this zone, the particle content has more dominant effect.

4.4 Bar–particles coupled effect on dynamic stability of suspensions in the vertical direction

The vertical dynamic segregation can be defined as the migration of the particles from the top layer towards the bottom layer. As presented in Fig. 3, the thickness of both the bottom and middle layers is 3 cm, and the remaining thickness ($Z > 6$ cm) corresponds to the

top layer. Accordingly, the vertical dynamic segregation index (V.D.S.I.) can be defined as the ratio of the spread in particle contents of the top and bottom layers to the initial particle content, as follows:

$$\text{V.D.S.I.} = \frac{\text{Particle content @ bottom layer} - \text{Particle content @ top layer}}{\text{Initial mean particle content}} \quad (6)$$

The results of vertical dynamic segregation index values obtained for the suspensions with 4.6% and 8.7% particle contents in presence of two bar arrangements (3 and 18 bars) are summarized in Table 1.

As can be observed, for a given bar arrangement, increasing the particle content can lead to lower vertical dynamic segregation. This can be explained by the lattice effect resulting in creation of an internal structure of solid particles in a multiphase material [26–28]. Indeed, once the particles settle down to the bottom segment of the L-Box, they create an internal structure which can resist other particles that were supposed to segregate. Increasing the initial particle content can result in strengthening this mentioned internal structure and, therefore, leading to decrease in vertical dynamic segregation. On the other hand, as can be observed in Table 1, for a given particle content, increasing the number of bars can reduce the vertical dynamic segregation. This can be due the auxiliary effect of obstacles to the lattice performance of the settled particle. Indeed, increasing obstacles prevent the motion of more particles towards bottom layer and works as a sieve. This can be described as the blocking in the vertical direction. Therefore, the minimum V.D.S.I. value of 0.80 was obtained for the highest particle content of 8.7% and the maximum number of bars (i.e., 18).

Table 1 Vertical dynamic segregation indices of 4.6% and 8.7% particle contents and numbers of obstacles (3 and 18 bars)

Particle content (%)	Number of obstacles	
	3	18
4.6	V.D.S.I. = 1.06	V.D.S.I. = 0.94
8.7	V.D.S.I. = 0.97	V.D.S.I. = 0.80

5 Conclusions

In this paper, a CFD software was employed to evaluate the coupled effect of reinforcing bars and the concentration of relatively large particle (20 mm) on flow performance of SCC cast in an L-Box test set-up. The L-Box had three numbers of 0, 3, and 18 bars distributed along the horizontal channel. Modelling of the L-Box set-up without any obstacles resulted in the evaluation of pure particle effect on non-restricted flow. On the other hand, the presence of 3 and 18 reinforcing bars corresponded to 0.7% and 4% of area of concrete in XY plane of the horizontal channel, that correspond low and highly congested flows, respectively. The CFD modellings was employed successfully to simulate the dynamic segregation and blocking phenomena of the investigated suspension in the L-Box test set-up. The CFD software was shown to be able to enable qualitative simulation the behavior of a non-Newtonian fluid interacting with solid particles, using the VOF method. Solving the Navier–Stokes equation by the CFD software made it possible to track the position and displacements of the solid particles, which their advections were provided by the suspending fluid. Segregation and blocking phenomena are only calculated for a portion of suspended coarse aggregates, which is actually less than typical contents of coarse aggregates in SCC (i.e., 10–30%). Indeed, it was assumed that the aggregate fraction that can remain in homogeneous suspension during the flow period can be considered as part of the homogeneous suspending fluid. The modelled materials consisted of a suspending fluid, having moderate plastic viscosity of 25 Pa s, and high yield stress of 75 Pa s. The suspensions also consisted of two different contents of the single size solid spherical particles (4.6% and 8.7%, by volume) having a mono size of 20 mm in diameter and a density of 2500 kg/m^3, which is the same as the suspending fluid. It must be noted that these selected coarse particle contents of 20-mm diameter particles correspond to the volume fraction of the aggregate in SCC that have the highest

risk to segregate during flow leading to reduction in dynamic stability. Shear-induced dynamic segregation of the investigated suspensions was evaluated by the comparison of the particle content in each section to the last sampling part. Turgut et al. [11] showed experimentally that dynamic segregation and blocking can lead to lower coarse aggregate content in the last horizontal section of the L-Box set-up compared to that observed in the beginning of the horizontal channel.

The core of the study is statistic evaluation of the results obtained by numerical simulations of L-Box test. The main novelty of the paper is the methodology of estimating the degree of segregation depending on the parameters under investigation, including particle content and number of reinforcing bars. The concluding remarks can be expressed by the effects of the initial particle content of the suspension and configuration of reinforcement bars, as well as the interactions between particles and obstacles on passing ability, and dynamic stability of SCC as a heterogeneous material, as follows:

- A new approach is proposed to evaluate the bar–particles coupled effect on the horizontal dynamic stability and risk of blocking in three different interaction zones. These zones indicate parallel and opposite interactions between bars and particles which affect the flow performance of the investigated suspensions, as follows. Increasing both the particle content of the simulated concrete suspension and the number of bars in the L-Box horizontal section can lead to greater possibility of formation of particle arches, which increases the risk of blocking. These conclusions are in good agreement with the experimental and statistical results obtained by Yahia et al. [13] which showed that in order to reach a given level of passing ability, when the content of coarse aggregate increased, the number of reinforcing bars can decrease (i.e., higher clear distance between the obstacles). Nepomuceno et al. [12] also showed experimentally that in order to achieve a given level of self-compactability, in the case of higher number of reinforcing bars, the volumetric content of coarse aggregate needs to be reduced. On the other hand, as reported by Yahia et al. [13], the increase in particle content can lead to an increase in the overall viscosity and yield stress values of the suspension. Regarding the vertical variation of velocity of free surface flow of a suspension's layer [29], it can lead to lower relative velocity between the surrounding fluid and suspended solid particles. This can then improve the dynamic stability of the mixture in the horizontal direction.
- The numerical simulation results showed that in a given rheological properties of the suspending fluid (i.e., stable and homogeneous portion of the concrete), increasing both the particle content and number of reinforcing bars can increase dynamic segregation and blocking of the mixture through the horizontal channel of the L-Box by values of up to 2.5 and 3.2, respectively. The maximum horizontal dynamic segregation index (I.H.D.S.I.) was 5.5 for the suspension with the higher coarse aggregate content of 8.7% in the presence of 18 bars.
- The highest bar effect was observed in the middle horizontal section, which exhibited the maximum dynamic segregation compared to concrete sampled from sections located at the end of the horizontal channel. On the other hand, in the case of the highest particle content and the maximum number of obstacles, the effects of bars and particle content in the terminal horizontal parts decreased.
- In the case of casting of the SCC mixtures consisting of high concentrations of coarse aggregates in highly reinforced horizontal formworks, the effect of particle content and configurations of bars on passing ability and dynamic segregation of SCC are shown to be dominant in the middle horizontal sections. However, flow performance properties of SCC in the extreme sections located beneath the casting point and at the end of the formwork are found to depend mostly on the casting flow rate and length of formwork, respectively.
- The numerical simulation showed that unlike the horizontal dynamic segregation, increasing both particle content and density of reinforcing bars can decrease the vertical dynamic segregation index (up to 0.26).
- An auxiliary lattice effect on the motion of the particles was observed in the vertical compartment of the L-Box with a decrease in dynamic segregation index of up to 0.09.

Acknowledgements The authors wish to thank the financial support of the National Science and Engineering Research Council of Canada (NSERC) and the 16 industrial partners participating in the NSERC Chair on High Performance Flowable Concrete with Adapted Rheology, held by Professor Kamal H. Khayat of the Université de Sherbrooke.

Compliance with ethical standards

Conflict of interest The authors declare that they have no conflict of interest.

References

1. ACI Committee 237 (2007) Self-consolidating concrete, ACI 237R-07. American Concrete Institute, Farmington Hills
2. Khayat KH, Mitchell D (2009) Self-consolidating concrete for precast, prestressed concrete bridge elements. National Cooperative Highway Research Program, NCHRP Report 628. Transporation Research Board of the National Academies
3. Roussel N (2012) Understanding the rheology of concrete, 1st edn. Woodhead Publishing, Sawston. ISBN 9780857090287
4. Thrane LN (2007) Form filling with self-compacting concrete. Ph.D. Dissertation, Danish technological institute
5. Khayat KH (1999) Workability, testing, and performance of self-consolidating concrete. ACI Mater J 96(3):346–353
6. Khayat KH (1998) Use of viscosity-modifying admixture to reduce top-bar effect of anchored bars cast with fluid concrete. ACI Mater J 95(2):158–167
7. Sonebi M, Grünewald S, Walraven J (2007) Filling ability and passing ability of self-consolidating concrete. ACI Mater J 104(2):162–170
8. EFNARC (2002) Specification and guidelines for self-compacting concrete. EFNARC, Norfolk. ISBN 0-9539733-4-4
9. Nguyen TLH, Roussel N, Coussot P (2006) Correlation between L-box test and rheological parameters of a homogeneous yield stress fluid. Cem Concr Res 36:1789–1796
10. Lashkarbolouk H, Chamani MR, Halabian AM, Pishevar AR (2013) Viscosity evaluation of SCC based on flow simulation in the L-box test. Mag Concr Res 65(6):365–376
11. Turgut P, Turk K, Bakirci H (2012) Segregation control of SCC with a modified L-box apparatus. Mag Concr Res 64(8):707–716
12. Nepomuceno MCS, Preira-de-Oliveira LA, Lopes SMR, Franco RMC (2016) Maximum coarse aggregate's volume fraction in self-compacting concrete for different flow restrictions. Constr Build Mater 113:851–856
13. Yahia A, Khayat KH, Sayed M (2012) Statistical modelling of the coupled effect of mix design and rebar spacing on restricted flow characteristics of SCC. Constr Build Mater 37:699–706
14. Roussel N, Geiker MR, Dufour F, Thrane LN, Szabo P (2007) Computational modeling of concrete flow: general overview. Cem Concr Res 37:1298–1307
15. Yammine J, Chaouche M, Guerinet M, Moranville M, Roussel N (2008) From ordinary rheology concrete to self compacting concrete: a transition between frictional and hydrodynamic interactions. Cem Concr Res 38:890–896
16. Roussel N, Gram A, Cremonesi M, Ferrara L, Krenzer K, Mechtcherine V, Shyshko S, Skocec J, Spangenberg J, Svec O, Thrane LN, Vasilic K (2016) Numerical simulations of concrete flow: a benchmark comparison. Cem Concr Res 79:265–271
17. Shen L, Struble L, Lange DA (2009) Modeling dynamic segregation of self-consolidating concrete. ACI Mater J 106(4):375–380
18. Spangenberg J, Roussel N, Hattel JH, Stang H, Skocek J, Geiker MR (2012) Flow induced particle migration in fresh concrete: theoretical frame, numerical simulations and experimental results on model fluids. Cem Concr Res 42:633–641
19. Spangenberg J, Roussel N, Hattel JH, Sarmiento EV, Zirgulis G, Geiker MR (2012) Patterns of gravity induced aggregate migration during casting of fluid concretes. Cem Concr Res 42:1571–1578
20. Vasilic K, Schmidt W, Kühne HC, Haamkens F, Mechtcherine V, Roussel N (2016) Flow of fresh concrete through reinforced elements: experimental validation of the porous analogy numerical method. Cem Concr Res 88:1–6
21. Hirt CW, Nichols BD (1981) Volume of fluid (VOF) method for the dynamics of free boundaries. J Comput Phys 39(1):201–225
22. Hosseinpoor M, Khayat KH, Yahia A (2016) Numerical simulation of self-consolidating concrete flow as a heterogeneous material in L-box set-up—effect of rheological parameters on flow performance. Cem Concr Composites
23. Vanhove Y, Djelal C (2013) Friction mechanisms of fresh concrete under pressure. Int J Civil Eng Technol (IJCIET) 4(6):67–81
24. FLOW-3D user guide. www.flow3d.com
25. RILEM State of the Art Report, Technical Committee 222-SCF (2014) Simulation of fresh concrete flow. Springer, Imprint. ISBN 978-94-017-8883-0
26. Körner C, Thies M, Hofmann T, Thürey N, Rüde U (2005) Lattice Boltzman model for free surface flow for modeling foaming. J Stat Phys 121(1):179–196
27. Man H-K, van Mier JGM (2011) Damage distribution and size effect in numerical concrete from lattice analyses. Cement Concr Compos 33:867–880
28. Eliáš J, Stang H (2012) Lattice modeling of aggregate interlocking in concrete. Int J Fract 175(1):1–11
29. Thrane LN (2007) Form filling with self-compacting concrete. Ph.D. thesis, Danish Technological Institute